Hindawi
International Journal of Aerospace Engineering
Volume 2021, Article ID 5539401, 9 pages
https://doi.org/10.1155/2021/5539401

Research Article

Study on the Fast Extension Mechanism of Double-Cavity Shock Absorber with High-Pressure Piston

Xingbo Fang[1], **Hu Chen**[1], **Xiaohui Wei**[1,2] **and Hong Nie**[1,2]

[1]*College of Aerospace Engineering, Nanjing University of Aeronautics and Astronautics, Nanjing, Jiangsu 210016, China*
[2]*State Key Laboratory of Mechanics and Control of Mechanical Structures, Nanjing, Jiangsu 210016, China*

Correspondence should be addressed to Xiaohui Wei; wei_xiaohui@nuaa.edu.cn

Received 22 January 2021; Revised 1 April 2021; Accepted 7 April 2021; Published 22 April 2021

Academic Editor: Mohammad Tawfik

Double-cavity shock absorber with high-pressure piston is the core component of the nose landing gear of the carrier-based aircraft, and its fast-extension performance seriously affects the safety of the catapult-assisted takeoff. The design of a carrier-based aircraft in our country is carried out based on the traditional method of fast-extension dynamics, and it is found that the fast-extension capability is larger than designed. This paper analyzes the working principle of the high-pressure piston shock absorber and explains that the high-pressure air cavity pushes the piston rod to extend rapidly, which will cause the cavitation phenomenon in the main oil chamber. Thus, the cavitation in the main oil chamber makes the traditional modeling method of oil-liquid resistance force no longer applicable. Then, the axial force modeling method of shock absorber considering the cavitation effect is proposed. Based on the carrier-based aircraft, the dynamic response of the shock absorber in the process of fast extension is calculated and then it is compared with the calculation results of the traditional dynamic method. It is found that due to the cavitation effect caused by the forced fast extension section of the high-pressure air plug shock absorber, the fast extension work increases by 67.6%, thus, revealing the fast extension mechanism of the double-chamber shock absorber with high-pressure piston and successfully explaining the phenomenon of the fast extension ability exceeding the expectation of the shock absorber.

1. Introduction

The shock absorber is the key component of the aircraft landing gear. For catapult carrier-based aircraft [1], the shock absorber should not only meet the landing shock absorber requirements of carrier-based aircraft but also the catapult fast-extension performance. Therefore, the double cavity shock absorber with high-pressure piston which can meet the above contradictory functional requirements is one of the common configurations of the nose landing gear of carrier-based aircraft.

The dynamic characteristic analysis of the shock absorber is very important in the landing gear design. As early as 1951, Walls studied the parameter range of the variable index of air spring force [2] and contraction coefficient of oil hole [3] through the landing gear drop test. In 1976, Wahi studied the gas dissolution in the oil and the influence of oil compressibility on the dynamic characteristics of the shock absorber [4], and he also established a drop dynamic model including the dynamic characteristics of the shock absorber as well as the spin-up and spring back of the tire [5]. In 2009, Karam established the dynamic model of landing gear including the pressure of each cavity of shock absorber, the compressibility of oil, and the heat exchange between oil and gas [6], which has been verified by experiments. Chen et al. [7] found the abnormal fluctuation of vertical load in the landing gear drop test and judged that there was cavitation in the main oil chamber. Through theoretical calculation and laboratory test, it was proved that the existence of cavitation in the main oil chamber affects the landing gear shock absorber efficiency. Shin [8] used Adams to establish the dynamic model of single cavity shock absorber landing gear with cavitation effect, which proved that the simulation results were more consistent with the experimental results when the cavitation effect was taken into consideration.

The internal structure of the double-chamber shock absorber with high-pressure piston is complex, and the dynamic process of its fast extension is in the backward

stroke, which is obviously different from the landing shock absorber.

Theoretical and experimental studies have been carried out on the dynamic characteristics of the nose landing gear of carrier-based aircraft. Shen and Huang [9] [10] established the dynamic model of fast extension of the dual cavity shock absorber of landing gear and optimized the oil needle section of the shock absorber. Liu and Li [11] obtained the landing gear double cavity shock absorber performance sample by ADAMS simulation analysis and established the surrogate model by using the nonlinear response surface method to optimize the landing gear dual cavity shock absorber performance. Zhang et al. [12] optimized the parameters of the landing gear dual cavity shock absorber by comprehensively considering the landing gear double cavity shock absorber's landing shock absorber and fast-extension performance. Dou et al. [13] and Liu and Cui [14] carried out an experimental study on the fast extension process of landing gear with double cavity shock absorber, studied the influence of internal structure and filling parameters of shock absorber on the fast extension performance, and pointed out that the improvement of shock absorber performance would be accompanied by the decrease of shock absorber efficiency.

In the above research on nose landing gear nose extension performance, the air spring force and oil damping force of shock absorber are modeled by traditional hydropneumatic shock absorber dynamics.

The design of a carrier-based aircraft is carried out according to the traditional method of fast extension dynamics, and it is found that the fast extension capability is larger than designed. Based on the study of the working condition of each cavity of the high-pressure piston shock absorber, it is found that the negative pressure appears in the main oil chamber of the shock absorber during the fast extension process, resulting in the cavitation phenomenon, which leads to the invalidity of some assumptions in the modeling method of force elements such as oil resistance force in the traditional method of fast extension dynamics. Then, the dynamic pressure modeling method of each cavity in the shock absorber based on the elastic oil model is proposed, and the axial force calculation model of high-pressure air plug shock absorber considering the cavitation effect is established. Finally, the dynamic analysis of the nose landing gear fast extension process is carried out.

2. Working Principle of High-Pressure Air Plug Shock Absorber and Causes of Cavitation

The internal structure of the double chamber shock absorber with high-pressure piston is shown in Figure 1(a). The shock absorber is mainly composed of high-pressure piston (1), piston retaining ring (2), side oil hole (3), main oil hole (4), and piston rod (5). Compared with the single chamber shock absorber shown in Figure 1(b), the shock absorber with high-pressure piston has added high-pressure piston and piston retaining ring. Each component of the shock absorber divides the internal space into four chambers, namely, high-pressure gas chamber (6), low-pressure gas chamber (7), side oil chamber (8), and main oil chamber (9). Compared with the single chamber shock absorber, high-pressure gas chamber is added.

Figure 2 shows the force analysis of shock absorber with high-pressure piston and conventional shock absorber in the piston extension. The compressed gas in the gas chamber of the conventional shock absorber (Figure 2(b)) compresses the oil in the gas chamber downward, and the oil flows to the main oil chamber through the main oil hole, squeezing the end face of the piston rod, so as to push the piston rod to extend outwards. In this process, the oil in the shock absorber remains squeezed, and there will be no negative pressure and cavitation. However, Figure 2(a) shows that there is a high-pressure gas cavity in the shock absorber of medium and high-pressure piston. The piston rod is directly squeezed through the high-pressure piston downward (forced fast extension) to push the piston rod to extend outward. Due to the high air pressure in the high-pressure air chamber, the piston rod extends and the volume of the main oil chamber increases rapidly. The flow of oil into the main oil chamber under the action of the pressure in the low-pressure chamber is not enough to fill the main oil chamber. Consequently, a negative pressure appears when the pressure of the main chamber drops, which causes the dissolved gas in the oil to expand and form cavitation.

3. Traditional Modeling Method of Oil Damping Force and Its Problems

The traditional modeling method of the main oil hole resistance force F_{oz} of conventional hydropneumatic shock absorber is as follows.

$$F_{oz} = \frac{\rho A_{oz}^{3}}{2(C_{dz}A_{hz})^{2}}\dot{s}|\dot{s}|, \tag{1}$$

where ρ is oil density, A_{oz} is oil pressure area of main oil chamber, C_{dz} is shrinkage coefficient of main oil hole, A_{hz} is area of main oil hole, and s is compression capacity of shock absorber.

When the shock absorber piston rod is extended, $\dot{s}$ and F_{oz} both are negative, then, the above formula can be arranged as follows.

$$-C_{dz}A_{hz}\sqrt{-\frac{2}{\rho}\frac{F_{oz}}{A_{oz}}} = A_{oz}\dot{s}. \tag{2}$$

Meanwhile, according to the thin-walled hole flow algorithm [15], the flow formula of oil flowing through the shock absorber main oil hole during the piston rod extension can be written as follows:

$$q_z = -C_{dz}A_{hz}\sqrt{-\frac{2}{\rho}(P_z - P_d)}, \tag{3}$$

where q_z represents the oil flow of the main oil hole (the flow from the main oil chamber to the low-pressure chamber

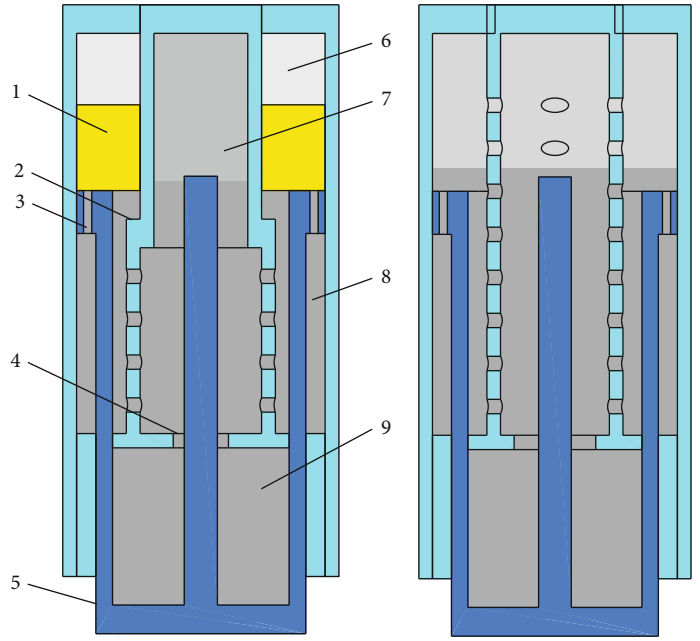

Figure 1: Structure diagram of shock absorber.

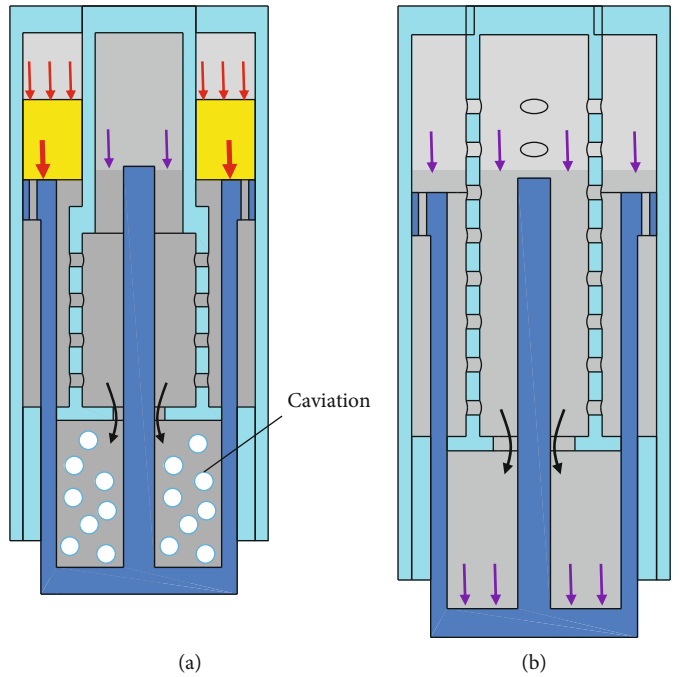

Figure 2: Force analysis of shock absorber.

is positive), P_d is the pressure of the low-pressure gas chamber, and P_z is the pressure of the main oil chamber.

From the analogy between formulas (2) and (3), it can be concluded that the oil damping force in formula (1) can represent the force generated by the pressure difference on the main pressure oil area. The difference is caused by the flow rate corresponding to the volume change rate of the main oil chamber flowing through the main oil hole. Then, the premise of the modeling method in formula (1) is that the volume change rate of the main oil chamber is equal to the flow rate of the main oil hole.

$$q_z = A_{oz}\dot{s}. \tag{4}$$

However, when cavitation occurs in the main oil chamber, as shown in Figure 2(a), the cavitation occupies a part

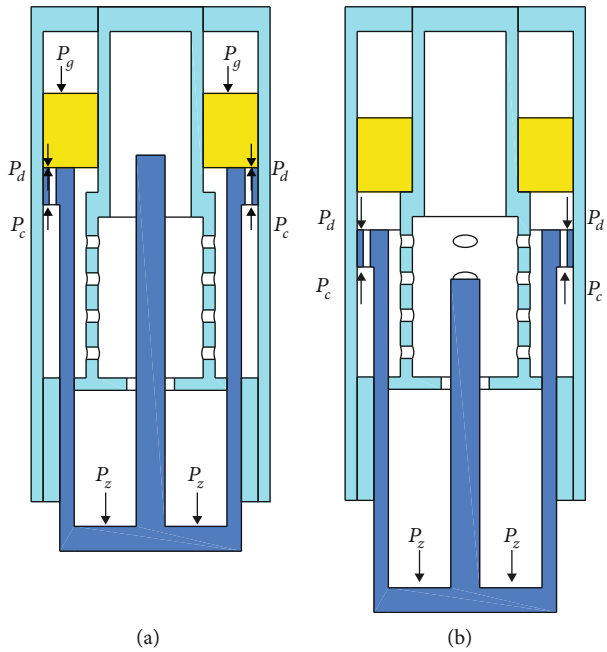

Figure 3: Force analysis of piston rod.

of the volume of the main oil chamber. According to the assumption of formula (4), the flow rate of the main oil hole is larger than the actual flow rate, so it can be concluded the oil damping force calculated by formula (1) is larger than the actual situation.

4. Axial Force Model of Shock Absorber considering Cavitation Effect

For the purpose of studying the influence of cavitation effect on the calculation results of reverse stroke axial force of the shock absorber with high-pressure piston, the following work has been carried out. Based on the principle of the shock absorber, the force analysis of the shock absorber piston rod was carried out, and the calculation model of axial force of shock absorber was established by dynamically calculating the pressure of each chamber in shock absorber considering cavitation effect.

4.1. Force Analysis of Shock Absorber Piston Rod. When the high-pressure piston shock absorber works in reverse stroke, it first goes through the high-pressure stroke condition, as shown in Figure 3(a), and then goes through the low-pressure stroke condition, as shown in Figure 3(b). In Figure 3, the mechanical behaviors of piston rod in high-pressure stroke condition and low-pressure stroke condition are different. As a result, the axial force of shock absorber is calculated in low-pressure condition and high-pressure condition separately.

$$F_h = \begin{cases} F_{\text{hd}} & s \le s_d, \\ F_{\text{hg}} & s > s_d, \end{cases} \tag{5}$$

where s_d is the stroke of shock absorber low-pressure structure.

As shown in Figure 3(a), during the high-pressure stroke condition, the piston rod is affected by the pressure of high-pressure gas chamber, low-pressure gas chamber, main oil chamber, and side oil chamber. The expression of resultant force along the axial direction of shock absorber is as follows.

$$F_{\text{hg}} = (P_g - P_d)A_g + (P_d - P_c)(A_d - A_h) + P_d(A_h - A_z) + P_z A_z, \tag{6}$$

where P_g is the pressure of high-pressure gas chamber, P_d is the pressure of low-pressure gas chamber, P_z is the oil pressure of main oil chamber, P_c is the oil pressure of side oil chamber, A_g is the annular cross-sectional area of high-pressure piston, A_d is the cross-sectional area of low-pressure gas chamber, A_z is the cross-sectional area of main oil chamber, and A_h is the external cross-sectional area of piston rod.

The axial force on the piston rod during the low-pressure stroke condition of the shock absorber is shown in Figure 3. The piston rod is separated from the high-pressure piston and only bears the pressure of the low-pressure gas chamber, main oil chamber, and side oil chamber. The expression of the shock absorber force on the piston rod is as follows.

$$F_{\text{hd}} = (P_d - P_c)(A_d - A_h) + P_d(A_h - A_z) + P_z A_z. \tag{7}$$

4.2. Calculation Model of Shock Absorber Chamber Pressure. The calculation error of traditional modeling method (1) of oil damping force lies in the assumption that the flow rate of main oil hole is equal to the volume change rate of main oil chamber. Taken the cavitation effect into consideration, the flow rate of main oil hole needs to be calculated by the pressure difference on both sides of oil hole. To calculate

the oil hole flow, the internal pressure of each cavity should be calculated according to the dynamic state of oil elastic modulus.

In equation (7), the calculation expression of the pressure in the low-pressure chamber is as follows.

$$P_d = (P_{d0} + P_{\text{atm}}) \left(\frac{V_{d0}}{V_{d0} + s_g A_g - s(A_d - A_z) - \int (q_z + q_c)} \right)^{\gamma_d} - P_{\text{atm}}, \tag{8}$$

where the expression of high-pressure piston stroke is defined below.

$$s_g = \begin{cases} 0 & s \le s_d, \\ s - s_d & s > s_d. \end{cases} \tag{9}$$

In equation (6), the calculation expression of high-pressure gas chamber pressure is as follows.

$$P_g = \left(P_{g0} + P_{\text{atm}}\right) \left(\frac{V_{g0}}{V_{g0} - s_g A_g} \right)^{\gamma_g} - P_{\text{atm}}. \tag{10}$$

In equation (7), without considering the elastic deformation of the piston rod, the expression of the time derivative of the oil pressure P_z in the main oil chamber is defined below.

$$\frac{dP_z}{dt} = \frac{\dot{s} A_z - E_z q_z}{V_{z0} - s A_z}, \tag{11}$$

where V_{z0} is the initial volume of the main oil chamber under the fully extended shock absorber state, E_z is the bulk modulus of the oil in the main oil chamber, and q_z is the flow rate of the main oil chamber flowing to the low-pressure gas cavity through the main oil hole.

The expression of oil bulk modulus E in oil chamber [15] is as follows.

$$E = E_l \frac{1 + \alpha (P_{\text{atm}}/P_{\text{atm}} + P)^{1/\gamma_o}}{1 + \alpha E_l \left(P_{\text{atm}}^{1/\gamma_o} / \gamma_o (P_{\text{atm}} + P)^{\gamma_o + 1/\gamma_o} \right)}, \tag{12}$$

where E_l is the bulk modulus of pure oil, α is the volume content of gas in the oil, γ_o is the polytropic index of gas in the oil, and P is the oil pressure in the oil chamber.

In equation (7), the expression of the time derivative of the oil pressure in the side oil chamber is as follows.

$$\frac{dP_c}{dt} = -\frac{\dot{s} A_c + E_c q_c}{V_{c0} + s A_c}, \tag{13}$$

where V_{c0} is the initial volume of the side oil chamber, E_c is the volume modulus of the oil in the side oil chamber, and q_c is the flow rate of the side oil cavity flowing to the low-pressure gas cavity through the side oil hole.

4.3. Flow Calculation Model of Damping Orifice. In equation (8), the expression of the flow rate of the main oil hole is as follows.

$$q_z = C_{\text{dz}} A_{\text{hz}} \text{ sign } (P_z - P_d) \sqrt{\frac{2|P_z - P_d|}{\rho}}. \tag{14}$$

In equation (11), the expression of side oil hole flow is as follows.

$$q_c = C_{\text{dc}} A_{\text{hc}} \text{ sign } (P_c - P_d) \sqrt{\frac{2|P_c - P_d|}{\rho}}, \tag{15}$$

where C_{dc} is the side oil hole shrinkage coefficient, and A_{hc} is the side oil hole area.

5. Analysis of Dynamic Response Results of Shock Absorber during Fast Extension

Based on the test method of nose landing gear in reference [13], this paper studies the fast extension performance of nose landing gear shock absorber with high-pressure air plug.

5.1. Dynamic Model of Nose Landing Gear Extension. The dynamic model of nose landing gear nose extension test method is modeled by two mass models [14]. Take the basket, counterweight, landing gear strut and strut as elastic mass, and shock absorber piston rod, wheel, and tire as inelastic mass. The dynamic equation is as follows.

$$\begin{aligned} m_{\text{tx}} \ddot{y}_{\text{tx}} &= F_h - m_{\text{tx}} g, \\ m_{\text{ft}} \ddot{y}_{\text{ft}} &= -k_v y_{\text{ft}} - F_h - m_{\text{ft}} g, \end{aligned} \tag{16}$$

where m_{tx} is the elastic support mass, m_{ft} is the inelastic support mass, y_{tx} is the elastic mass vertical displacement, k_v is the tire radial stiffness, y_{ft} is the inelastic mass vertical displacement, and g is the gravity acceleration.

The dynamic response model is used to calculate the dynamic response of the nose landing gear of a carrier-based aircraft in the fast extension. The total structural stroke of the nose landing gear shock absorber of the carrier-based aircraft is 550 mm, and the structural stroke of the low pressure is 350 mm. At the initial moment of nose landing gear extension, the shock absorber compression is 478 mm. The specific model parameters are shown in Table 1.

5.2. Calculation Results of Axial Force Component of Shock Absorber (Traditional Modeling Method). Figures 4 and 5 show the oil resistance force F_{oz} of main oil hole, air spring force F_{ad} of low-pressure air chamber, and air spring force F_{ag} of high-pressure air chamber in the process of fast extension using the traditional modeling method. The nose landing gear starts to extend at the zero point of the time axis. During the process of extension, the maximum reverse force F_{oz} of shock absorber is 52.5 kN at the time 0.091 s, and the corresponding F_{ad} value at this time is only 19.2 kN.

Table 1: Simulation parameters.

Symbol	Value	Symbol	Value
s_d	350 mm	P_{d0}	0.5 MPa
$s_{\max}$	550 mm	P_{g0}	5.5 MPa
m_{ft}	120 kg	k_v	1.7e6 N/m
m_{tx}	3360 kg	V_{d0}	3600 mL
s_0	478 mm	V_{g0}	1040 mL
g	9.82 m/s^2		

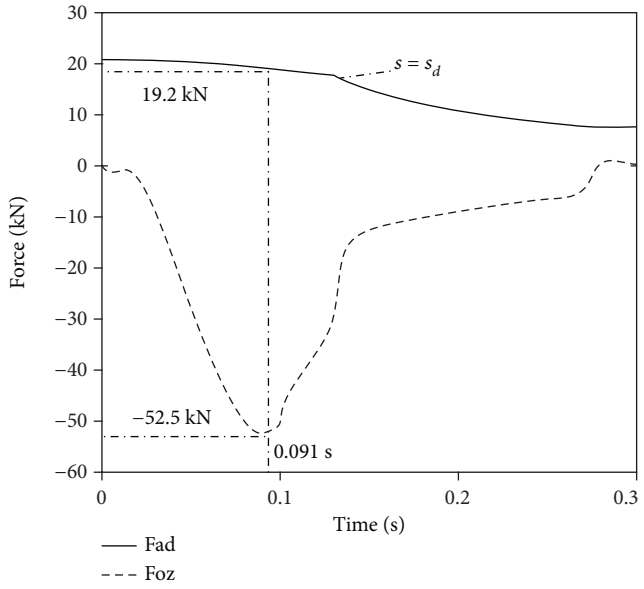

Figure 4: Time history of axial component force.

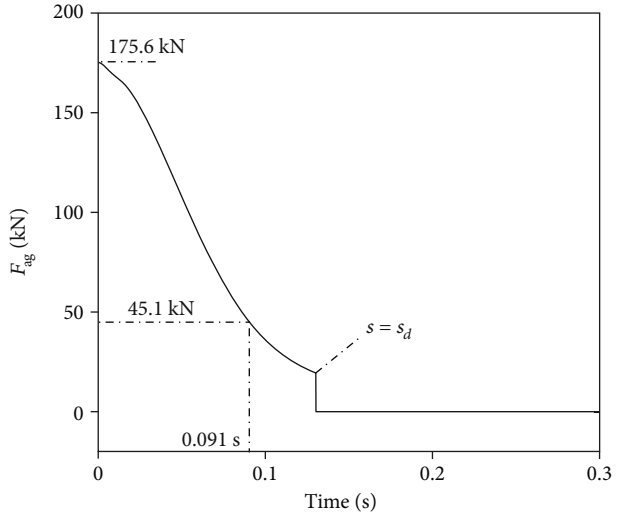

Figure 5: Time history of high-pressure cavity force.

According to the principle of oil resistance force of main oil hole, in the process of shock absorber elongation, the reverse damping force of main oil hole is generated when

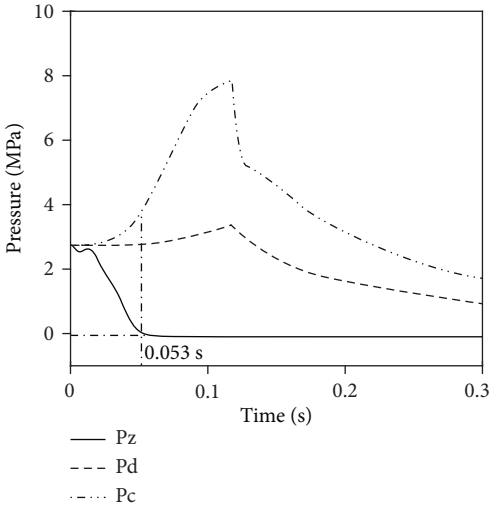

Figure 6: Cavity pressure of shock absorber.

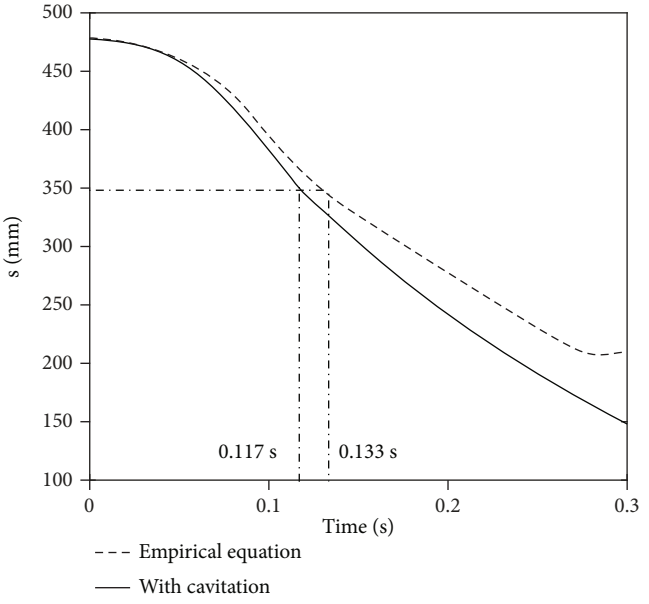

Figure 7: Comparison of shock strut stroke.

oil flows from low-pressure chamber through main oil hole to main oil chamber. As a result, the value of reverse damping force of main oil hole shall not be greater than that of air spring force of low-pressure chamber. From this, we can see that the results of main oil hole reverse damping force and low-pressure chamber air spring force are contradictory. The reason is that the damping force of the main oil hole is not produced by air spring force of high-pressure chamber at 45.1 kN (Figure 5), while the damping force is considered by traditional modeling method.

5.3. Comparison of Dynamic Response Calculation Results of Two Axial Force Models. Figure 6 shows the pressure change of each shock absorber chamber during the fast extension process calculated by the shock absorber model considering cavitation effect. From the pressure curve of the main oil chamber

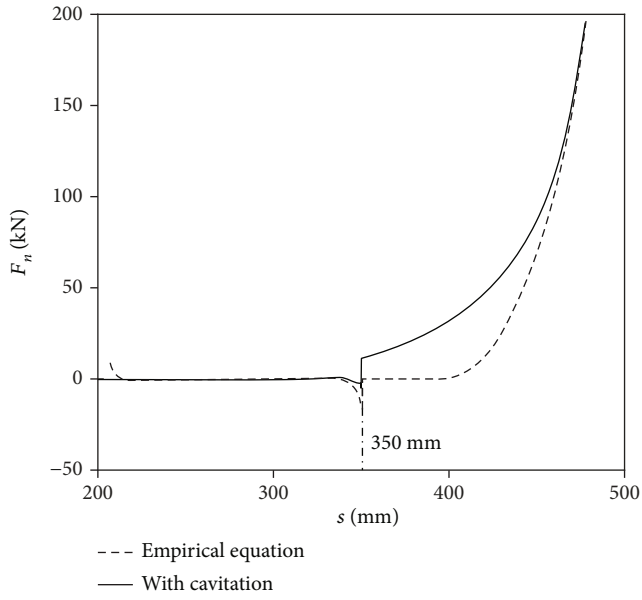

Figure 8: Comparison of efficiency diagrams.

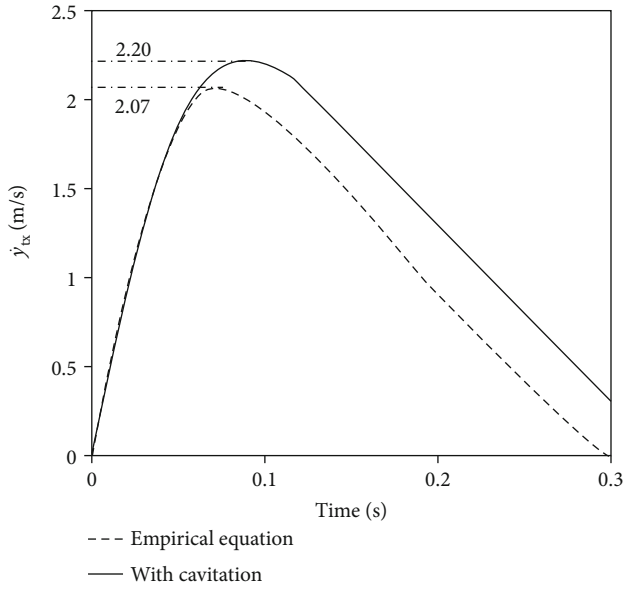

Figure 9: Comparison of vertical velocity of spring support mass.

in the figure, the pressure in the main oil chamber has been negative after 0.053 seconds, which indicates that cavitation has been existing in the main oil chamber after 0.053 s.

The comparison results of the axial stroke of the shock absorber calculated by two modeling methods of the nose landing gear during extension are given in Figure 7. It can be seen that there is obvious difference between the traditional modeling method and the shock absorber model with cavitation effect. The shock absorber model with cavitation effect reaches the fast extension at 0.1 s. However, it takes 0.130 s for the traditional modeling method to complete the high-pressure stroke. Moreover, due to the cavitation effect, the damping force of the main oil hole in the high-pressure stroke stage is

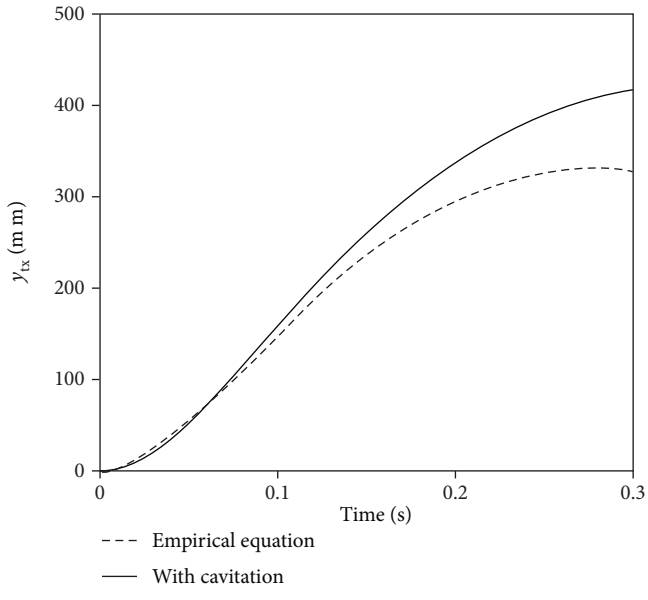

Figure 10: Comparison of vertical displacement of spring support mass.

invalid. The axial force calculated by the shock absorber model considering the cavitation effect is larger than that calculated by the traditional modeling method, and the work diagram of the shock absorber is also fuller (Figure 8). In Figure 8, the output work of the shock absorber model with cavitation effect is 9.05 kJ, while that of the shock absorber model with traditional modeling method is 5.40 kJ, with a difference of 67.6%.

In Figure 8, when the shock absorber is in the low-pressure stroke stage ($s < 350$ mm), there is no obvious difference in the axial direction calculated by the two modeling methods. The reason is that the working principle of the high-pressure piston shock absorber in the low-pressure stroke stage is not significantly different from that of the conventional single cavity shock absorber. It reveals that the traditional modeling method of oil damping force is accurate for the calculation of single cavity shock absorber.

Figure 9 shows the vertical velocity of elastic support mass during nose landing gear fast extension. The peak velocity value calculated by shock absorber model with cavitation effect is 2.20 m/s, while that calculated by traditional modeling method is 2.07 m/s, with a difference of 6.3%. At the same time, there are also obvious differences in the vertical displacement calculated by the two shock absorber modeling methods (Figure 10). At the time of 0.3 s, the elastic support mass displacement value calculated by the shock absorber model considering the cavitation effect is 416.5 mm, while that calculated by the traditional modeling method is 338.0 mm, with a difference of 23.2%.

6. Conclusions

(1) It is concluded that for the shock absorber with high-pressure piston, in the forced fast extension condition, the high-pressure air cavity pushes the piston rod to extend rapidly, which will cause the main oil chamber to appear negative pressure and lead to cavitation

(2) It is clarified that cavitation in the main oil chamber of the shock absorber high-pressure piston will lead to the hypothesis that the volume change rate of the main oil chamber is equal to the flow rate of the main oil hole, which is the premise of the traditional oil damping force modeling method for sudden extension dynamics

(3) Based on the elastic oil model, the dynamic pressure modeling method of each chamber in the shock absorber is proposed, and the axial force model considering cavitation effect is established to calculate the dynamic pressure change in each chamber

(4) Based on the study of the dynamics of the shock absorber axial force modeling method considering the cavitation effect, it is found that compared with the traditional modeling method, the output work of the fast extension is increased by 67.6%

Nomenclature

A_{oz}: Oil pressure area of main oil chamber
C_{dz}: Shrinkage coefficient of main oil hole
F_{oz}: Main oil hole resistance force
q_z: Oil flow of the main oil hole
P_z: Pressure of the main oil chamber.
P_g: Pressure of high-pressure gas chamber
A_g: Annular cross-sectional area of high-pressure piston
A_z: Cross-sectional area of main oil chamber
s_g: High-pressure piston stroke
E: Oil bulk modulus
α: Volume content of gas in the oil
P: Oil pressure in the oil chamber
E_c: Volume modulus of the oil in the side oil chamber
A_{hc}: Side oil hole area
m_{ft}: Inelastic support mass
y_{ft}: Inelastic mass vertical displacement
A_{hz}: Area of main oil hole
s: Compression capacity of shock absorber
ρ: Oil density
P_d: Pressure of the low-pressure gas chamber
s_d: Stroke of shock absorber
P_c: Oil pressure of side oil chamber
A_d: Cross-sectional area of low-pressure gas chamber
A_h: External cross-sectional area of piston rod
V_{z0}: Initial volume of the main oil chamber
E_l: Bulk modulus of pure oil
γ_o: Polytropic index of gas in the oil
V_{c0}: Initial volume of the side oil chamber
C_{dc}: Side oil hole shrinkage coefficient
m_{tx}: Elastic support mass
y_{tx}: Elastic mass vertical displacement
g: Gravity acceleration.

Data Availability

No data were used to support this study.

Conflicts of Interest

The authors declared that they have no conflicts of interest to this work.

Authors' Contributions

Xingbo Fang and Hu Chen are co-first authors.

References

[1] The Chief Committee of Aircraft Design Manual, *Aircraft design manual: takeoff and landing system design*, Aviation Industry Press, Beijing, 2002.

[2] J. H. Walls, *Investigation of the air-compression process during drop tests of an oleo-pneumatic landing gear, [NACA TN 2477]*, Langley Aeronautical Laboratory Langley Field, 1951.

[3] J. H. Walls, *An experiment study of orifice coefficients, internal structure pressure, and loads on a small oleo-pneumatic shock structure, [NACA TN 3426]*, Langley Aeronautical Laboratory Langley Field, 1955.

[4] M. K. Wahi, "Oil compressibility and polytropic air compression analysis for oleopneumatic shock struts," *Journal of Aircraft*, vol. 13, no. 7, pp. 527–530, 1976.

[5] M. K. Wahi, "Oleopneumatic shock strut dynamic analysis and its real-time simulation," *Journal of Aircraft*, vol. 13, no. 4, pp. 303–308, 1976.

[6] W. Karam and J. Mare, "Advanced model development and validation of landing gear shock struts," *Proceedings of the Institution of Mechanical Engineers, Part G: Journal of Aerospace Engineering*, vol. 224, no. 5, pp. 575–586, 2009.

[7] Y. Chen, H. Zheng, Y. He, and J. Cheng, "Study on landing gear drop dynamics with cavitation effect," *Journal of Nanjing University of Aeronautics & Astronautics.*, vol. 47, no. 4, pp. 602–606, 2015.

[8] L. Y. Shin, "Effects of cavitation and drop characteristics on oleo-pneumatic type landing gear systems," *Journal of The Korean Society Aeronautical and Space Sciences.*, vol. 37, no. 2, pp. 193–200, 2009.

[9] Q. Shen and H. Zaixing, "Optimization on fast-extension performance of nose landing gear of carrier-based aircraft," *Computer Aided Engineering.*, vol. 18, no. 3, pp. 31–36, 2009.

[10] Q. Shen, *Optimization to the Cross Section of Metering Pin in the Landing Gear Shock Absorber of Carrier-Based Aircrafts*, Nanjing university of acronautics and astronautics, Nanjing, 2009.

[11] L. Tianhui and L. Zanke, "Performance optimization of oleo-pneumatic damper with two air chambers," *Journal of Harbin University of Commerce (Natural Sciences Edition).*, vol. 30, no. 6, pp. 720–723, 2014.

[12] Z. Ming, N. Hong, and Z. He, "Optimization parameters of nose landing gear considering both take-off and landing performance of catapult take-off carrier-based aircraft," *Transactions of Nanjing University of Aeronautics & Astronautics.*, vol. 33, no. 2, pp. 187–198, 2016.

[13] D. Qingbo, C. Yi, X. Ma, and etc, "Experimental study on the sudden-extension performance of carrier-based aircraft landing gear," *Journal of Vibration Engineering.*, vol. 31, no. 1, pp. 102–109, 2018.

[14] L. Chongchong and C. Rongyao, "Analysis and test for extension performance of nose landing gear of carrier-based aircraft," *Mechanical Science and Technology for Aerospace Engineering.*, vol. 35, no. 11, pp. 1686–1690, 2016.

[15] N. D. Manring, *Hydraulic Control Systems*, John Wiley & Sons, New York, 2005.